ACS APPLIED MATERIALS & INTERFACES

Research Article

www.acsami.org

Adjusting the Ion Permeability of Polyelectrolyte Multilayers through Layer-by-Layer Assembly under a High Gravity Field

Chao Jiang,[†,‡] Caijun Luo,[‡] Xiaolin Liu,[‡] Lei Shao,[*,‡] Youqing Dong,[§] Yingwei Zhang,[†] and Feng Shi[*,†]

[†]State Key Laboratory of Chemical Resource Engineering & Key Laboratory of Carbon Fiber and Functional Polymer, Ministry of Education, Beijing University of Chemical Technology, Beijing 100029 China

[‡]State Key Laboratory of Organic−Inorganic Composites & Beijing Laboratory of Biomedical Materials, Beijing University of Chemical Technology, Beijing 100029 China

[§]College of Chemistry and Materials Engineering, Wenzhou University, Wenzhou 325027 China

Supporting Information

ABSTRACT: The layer-by-layer (LbL) assembled multilayer has been widely used as good barrier film or capsule due to the advantages of its flexible tailoring of film permeability and compactness. Although many specific systems have been proposed for film design, developing a versatile strategy to control film compactness remains a challenge. We introduced the simple mechanical energy of a high gravity field to the LbL assembly process to tailor the multilayer permeability through adjusting film compactness. By taking poly(diallyldimethylammonium chloride) (PDDA) and poly{1−4[4-(3-carboxy-4-hydroxyphenylazo)benzenesulfonamido]-1,2-ethanediyl sodium salt} (PAzo) as a model system, we investigated the LbL assembly process under a high gravity field. The results showed that the high gravity field introduced effectively accelerated the multilayer deposition process by 20-fold compared with conventional dipping assembly; the adsorption rate was positively dependent on the rotating speed of the high gravity equipment and the concentration of the building block solutions. More interestingly, the film compactness of the PDDA/PAzo multilayer prepared under the high gravity field increased remarkably with the growing rotational speed of the high gravity equipment, as demonstrated through comparisons of surface morphology, cyclic voltammetry curves, and photoisomerization kinetics of PDDA/PAzo multilayers fabricated through the conventional dipping method and through LbL assembly under a high gravity field, respectively. In this way, we have introduced a simple and versatile external form of mechanical energy into the LbL assembling process to improve film compactness, which should be useful for further applications in controlled ion permeability, anticorrosion, and drug loading.

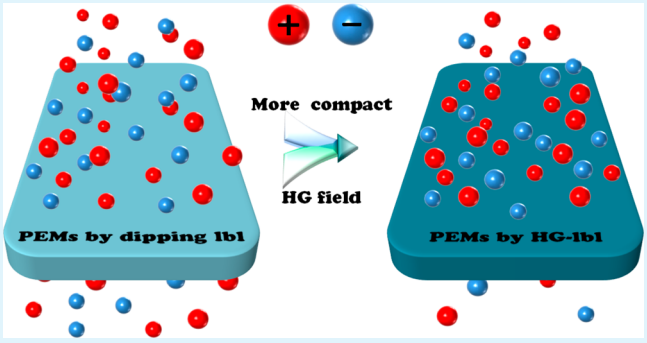

KEYWORDS: *layer-by-layer assembly, high gravity field, reduction of ion permeability, photoisomerization of Azo group, acceleration of diffusion process, improvement of film compactness*

INTRODUCTION

The layer-by-layer (LbL) assembled technique was initiated by Iler[1] and rediscovered by Decher,[2,3] and it has gained increasing attention as a simple and versatile method to fabricate ultrathin multilayered films at the nanoscale, with a flexible design in film composites and structures.[4,5] For decades, numerous multilayers have been well applied in various research fields for electronics,[6] optical films,[7] macroscopic supramolecular assembly,[8,9] superhydrophobic coatings,[10] biointerface,[11] drug delivery,[12] self-healing materials,[10] and so on.[13−17] Among the many film qualities to be tailored, film permeability is especially significant for further applications of multilayers in ion transportation,[18,19] water purification,[20,21] solvent separation,[22,23] as a gas barrier,[24,25] controlled loading and releasing,[26,27] and so on.

Currently, there are several strategies proposed to adjust the permeability of the multilayers, including selecting specific multilayers according to their inherent characteristics,[28] altering the deposited number of bilayers to control film thickness and porosity,[29,30] and introducing pH,[31] thermal,[32] photo,[33] or redox[34] responsive groups to change film morphology through external stimuli. For example, in the first strategy, multilayers with strong−strong polyelectrolytes demonstrated a relatively more compact morphology and low permeability than those composed of weak−weak polyelectrolytes,[28] which is useful as a barrier for anticorrosion applications. In the second strategy, due to the tailoring property of the LbL assembly process, the

Received: March 12, 2015
Accepted: May 8, 2015
Published: May 8, 2015

DOI: 10.1021/acsami.5b02179
ACS Appl. Mater. Interfaces 2015, 7, 10920−10927

permeability of multilayers are highly correlated with alternately deposited cycles.[29] In the third strategy, Rubner et al. have used multilayers with weak polyelectrolytes bearing amino or carboxylic acid groups and tuned film porosity by taking advantage of pH responsive swelling−deswelling properties of the multilayers.[31] Vancso and his co-workers has assembled polycation and polyanion, both bearing ferrocene groups, to be hollow capsules, which presented redox responsive behaviors of molecular permeability.[34] From the above strategies, we found that control over the compactness of the multilayer was one of the key factors to influence film permeability; the multilayer acted as a good barrier when its permeability was reduced with growing compact morphology.

Although the above methods allow tailoring of film permeability, they are usually limited to specific multilayers. Therefore, it is still a challenge to develop a versatile strategy to control film compactness because the compactness of nanothin films is significant to the property of ion permeability.[35−38] For example, Xu et al. interpreted the improved selective ion permeability of a cation exchange membrane with denser surface morphology after annealing process.[35] Tsukruk's group demonstrated the compaction of star polyelectrolytes to form LbL assembled microcapsule caused photo induced changes in microcapsule permeability, which could be useful for controlled loading/unloading.[36] Chang et al. reported that LbL assembled thermoresponsive microcapsules with more compact walls displayed better selective permeability to desired molecules, thus showing potential application for encapsulation of targeted species.[37] However, it is essential to be independent of special systems for the control of film compactness for desired permeability. Therefore, introducing a versatile mechanical field could be a simple and general solution to improving film quality,[5,39−42] which should be promising to adjust the film compactness and for further industrial applications.

The high gravity technique is a well-established industrial method to enhance mass and heat transfer rate in chemical engineering processes by providing mechanical energy with strong shear stress. With high gravity equipment, the solution could be broken into tiny droplets, threads, and thin films, and the flowing, distribution, and mixing processes of solutions could thus be accelerated by 1−3 orders of magnitude compared with normal conditions (Part 1 of Supporting Information). We were the first to introduce this industrial method into a layer-by-layer assembled process for the construction of multilayers containing polyethylenimine and zinc oxide nanoparticles.[40] By investigating the adsorption kinetics of the assembled building blocks, we demonstrated that the time to reach saturated adsorption could be shortened by 5-fold compared with adsorption under the conventional dipping process. This result was interpreted by the thinned boundary layer that hindered the diffusion and deposition of building blocks in the presence of the high gravity field, which contributed to accelerated adsorption of building blocks onto the substrate. Similar phenomena were also observed in the multilayer formation on nonplanar substrates.[41] We further proved that the high gravity field could be used to influence and adjust the LbL assembling behavior from exponential to linear film growth.[42] The strong shear force contributed to reducing surface roughness during the exponential buildup of multilayers and resulted in a multilayer with compact structures.

We therefore wondered whether we could apply LbL assembly under a high gravity field to tune multilayer permeability through adjusting film compactness. To demonstrate this issue, we investigated the LbL assembly process under a high gravity field by taking poly(diallyldimethylammonium chloride) (PDDA) and poly{1-4[4-(3-carboxy-4-hydroxyphenylazo)benzenesulfonamido]-1,2-ethanediyl sodium salt} (PAzo) as a model system. The results demonstrated that the high gravity field introduced effectively accelerated the multilayer deposition process by 20-fold compared with the conventional dipping assembly; the adsorption rate was positively dependent on the rotating speed of the high gravity equipment and the concentration of the building block solutions. More interestingly, the film compactness of the PDDA/PAzo multilayer prepared under the high gravity field increased remarkably with the growing rotational speed of the high gravity equipment, which was demonstrated through comparisons of the surface morphology, cyclic voltammetry curves and photoisomerization kinetics of PDDA/PAzo multilayers fabricated through the conventional dipping method and LbL assembly under a high gravity field, respectively.

EXPERIMENTAL SECTION

Materials and Instrument. The following chemicals were used as supplied: PDDA solution (20 wt% in H_2O, M_w 200 000−350 000) and PAzo were from Aldrich (St. Louis, MO), $[Ru(NH_3)_6]Cl_3$ from J&K Scientific Ltd. (Beijing, China), Tris(hydroxymethy)aminomethane (Tris) from Aladdin (Shanghai, China). H_2SO_4 (98%), H_2O_2 (30%), NaCl, KCl, HCl (37%), and $K_3[Fe(CN)_6]$ were purchased from Sinopharm Chemical Reagent Beijing Co. (Beijing, China).

The Tris buffer solution was prepared as follows: 2.42 g of Tris, 5.85 g of NaCl, and 0.372 g of KCl were dissolved in 1000 mL H_2O, and then the solution pH value was adjusted to 7 by HCl. The quartz substrates and silicon wafers used in all experiments were washed with piranha solution (a mixed solution of 98% H_2SO_4 and 30% H_2O_2 with a volume ratio of 7:3) and rinsed with deionized water, followed by drying in a N_2 flow.

CAUTION: *Piranha solutions are extremely corrosive; therefore, note that the piranha solutions were used in a fume hood with acid-resistant gloves.*

The high gravity equipment for HG-LbL assembly was homemade as illustrated in Scheme S1 (SI):[40] The inner diameter of the rotator is 20 mm, and the outer diameter is 50 mm. The internal and external widths of the rotator are 10 and 17 mm, respectively. Four slots (14 × 12 × 1 mm) are set in four directions inside of the rotator. The distributor consists of two pipes (5 × 1 mm), each with a hole of 1 mm diameter. The rotator is installed inside the fixed cavity with a diameter of 100 mm and rotates at a speed of several hundred to several thousand rotations per minute. The polyelectrolyte solutions are pumped into the cavity using a peristaltic pump (BT100-2J) from Baoding Longer Precision Pump Co., Ltd.

The multilayers deposited on quartz substrates were characterized by UV−visible spectroscopy on a Hitachi U-3900H spectrophotometer. AFM images of multilayers on silicon wafers were obtained on a Dimension 3100 instrument from Veeco (Plainview, NY). Cyclic voltammetry (CV) curves were obtained from CHI660E electrochemical workstation from Shanghai Chenhua Instruments Limited (Shanghai, China). UV light at a wavelength of 375 nm with a power of 3.0 mW/cm^2 was from an HTLD-4II UV-LED light source curing system (Shenzhen, China). Film thickness was measured with an ellipsometer (SE200BA, Angstrom Sun, Acton, MA).

Adsorption Kinetics of PAzo onto Substrate with PDDA. The cleaned quartz substrates were immersed in PDDA (aq, 1 mg/mL) for 30 min to modify the surface with PDDA groups, and then the substrate with PDDA was transferred to the PAzo solution (in Tris buffer with a pH value of 7, 0.01 mg/mL) for different time intervals. After each immersion time interval, the substrate absorbed with PAzo was detected through UV−visible spectra. For each obtained UV−visible curve, the absorbance at the strongest featured peak was

DOI: 10.1021/acsami.5b02179
ACS Appl. Mater. Interfaces 2015, 7, 10920−10927

correlated with the corresponding immersing time. The adsorption kinetics was thus plotted. For the adsorption kinetics under the conventional dipping method, the immersion process in PAzo was carried out at room temperature in a beaker; for the kinetics under high gravity, the substrate was inserted into a slot within the high gravity equipment (Scheme 1) and the PAzo solution was pumped with a rate of 30 mL/min into the equipment at a rotating speed of 2400 r/min, which was kept with different time interval to determine the adsorption kinetics.

Scheme 1. Illustration of LbL Assembly Process of PDDA/PAzo Multilayer under High Gravity Field[a]

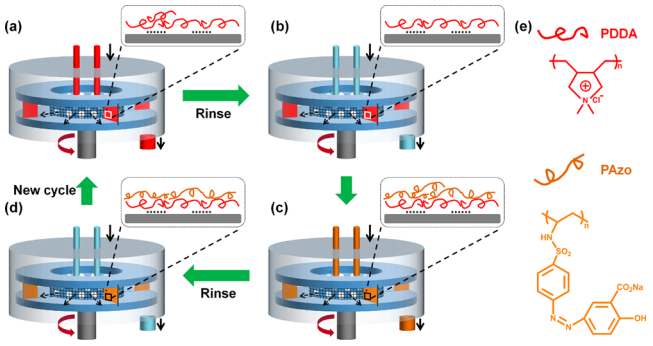

[a](a) The PDDA solution (red color) was pumped to the high gravity machine and deposited on the inserted substrates; (b) deionized water was pumped into the machine to wash excessive adsorption of PDDA; and (c) PAzo solution (brown color) was pumped into the machine followed by (d) rinsing. The cycle of a–d was repeated. (e) Structures and illustration of the used building blocks of PDDA and PAzo.

LbL Assembly of PDDA/PAzo Multilayer under Conventional LbL Assembly Process and High Gravity Field. The LbL assembly process of PDDA/PAzo was carried out as follows: the cleaned quartz substrate was pretreated by immersing in PDDA (aq, 1 mg/mL) for 30 min for a good modification of the first layer. The substrate was then alternately immersed in PAzo (in Tris buffer with a pH value of 7, 0.01 mg/mL) for 15 min and PDDA (aq, 1 mg/mL) for 10 min each until the desired number of bilayers, n, was achieved, which was noted as $(PDDA/PAzo)_n$ multilayer. After each deposition in solutions, the substrate was cleaned with copious water and dried in a nitrogen flow.

For the LbL assembly procedure under high gravity (Scheme 1), first the cleaned quartz substrates were inserted into the slots of the high gravity equipment. After the high gravity machine was turned on and reached the set rotating speed with a constant value (2400 r/min), the PDDA solution (aq, 1 mg/mL) was pumped in with a commercially available peristaltic pump (not shown) at a rate of 30 mL/min for 1 min as shown in Scheme 1a. Afterward, the high gravity equipment was kept rotating without any liquid for 1 min, then the substrate was cleaned through continually pumping deionized water into the equipment for 1 min and dried by keeping the equipment rotating for 1 min without any liquid. Second, the PAzo solution (in Tris buffer with a pH value of 7, 0.01 mg/mL) was pumped in for 3 min as shown in Scheme 1c, followed by identical washing and drying. Third, the alternate deposition of PDDA and PAzo was cycled. Note that the time exposed to high gravity field was calculated after the high gravity machine was started and reached set rotating speeds, which only took several seconds. If not specifically noted, the rotating speed of the high gravity equipment was kept at 2400 r/min, and the concentrations of PDDA and PAzo for both dipping assembly and assembly under the high gravity field were kept at 1 and 0.01 mg/mL.

Permeability of PDDA/PAzo Multilayer. Considering the flexibility when LbL assembly was under high gravity equipment, we used detachable gold electrodes to deposit multilayers for ion permeability testing through cyclic voltammetry (CV) mode with an electrochemical workstation. Both the anion label of $K_3[Fe(CN)_6]$ and cation label of $[Ru(NH_3)_6]Cl_3$ were used as probes. Prior to the modification and measurements, electrodes were carefully cleaned, then immersed in an ethanol solution of mercaptoacetic acid (0.1% v/v) overnight, followed by rinsing with ethanol; in this way, the surfaces of the electrodes were modified with acid groups, which contributed to the interactive groups with PDDA when in the LbL assembling procedure. After the LbL assembly procedure under either conventional dipping process or high gravity field, the gold electrodes were modified with $(PDDA/PAzo)_{10}$ multilayers. We used the three-electrode cell accessory as the container to hold $K_3[Fe(CN)_6]$ (aq, 1 mM, 0.1 M KCl) or $[Ru(NH_3)_6]Cl_3$ (aq, 2 mM, 0.1 M KCl) for solutions, the gold electrodes modified with $(PDDA/PAzo)_{10}$ multilayer as the working electrode, a platinum electrode as the counter-electrode and a Ag/AgCl electrode as the reference electrode for the electrochemical measurements. Under the CV testing mode of the electrochemical workstation, the scan rate was 0.1 V/s.

Photoisomerization of PDDA/PAzo Multilayer. A monochromatic light at a wavelength of 375 nm with an intensity of 3.0 mW/cm^2 was used to induce the photo isomerization of Azo groups: after being modified with 7 bilayers of PDDA/PAzo multilayer, the quartz plates were exposed to UV light for different time intervals; after each time interval, we characterized the isomerization kinetics of PAzo with UV–visible spectra.

RESULTS AND DISCUSSION

To confirm whether a high gravity field would influence the film quality of a PDDA/PAzo multilayer at the molecular level, we have investigated the adsorption kinetics of PAzo on the substrate bearing PDDA coating and the LbL assembling behaviors of PAzo and PDDA both with and without high gravity field. We considered the major driving force for the LbL assembly of PDDA and PAzo was electrostatic interaction because PDDA was a strong polycation while PAzo presented a carboxylic acid group in each repeated unit, which should be fully deprotonated at a pH value of 7 to favor for electrostatic interaction with PDDA. Under the conventional LbL assembly

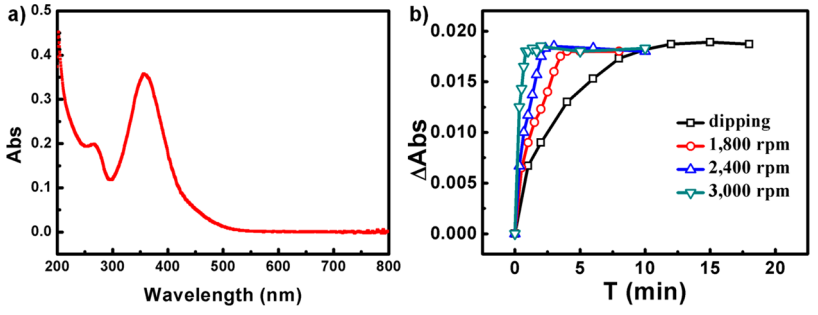

Figure 1. (a) UV–visible spectrum of PAzo aqueous solution (0.01 mg/mL); (b) adsorption kinetics of PAzo onto quartz substrate with PDDA under (black □) dipping condition and high gravity field with rotating speed of (red ○) 1800, (blue △) 2400, and (green ▽) 3000 r/min.

DOI: 10.1021/acsami.5b02179
ACS Appl. Mater. Interfaces 2015, 7, 10920–10927

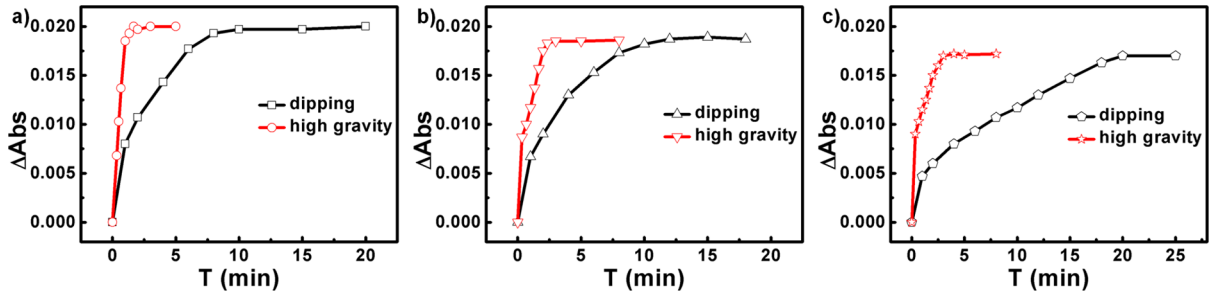

Figure 2. Adsorption kinetics of PAzo on the substrate with PDDA under (black) conventional dipping or (red) high gravity field conditions for PAzo solutions at different concentrations of (a) 0.02, (b) 0.01, and (c) 0.005 mg/mL, respectively.

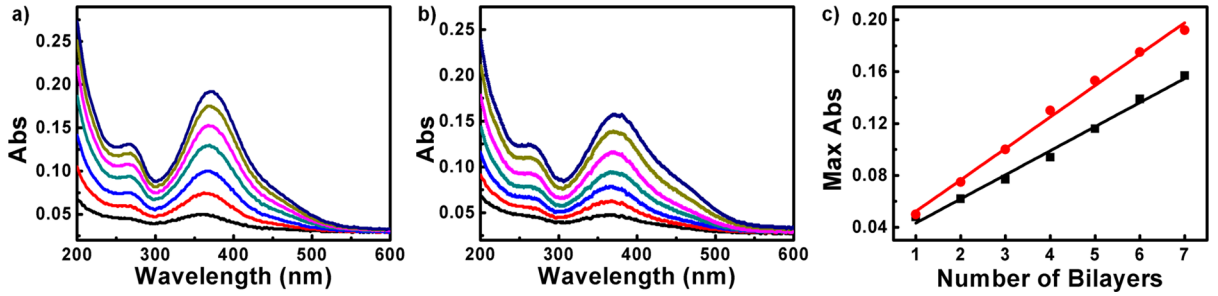

Figure 3. UV−visible spectra of PDDA/PAzo multilayer after deposition of every bilayer for (a) conventional LbL assembly process and (b) LbL assembly under high gravity field. (c) Linear correlation between the maximum featured peak absorbance of PAzo and the deposited number of bilayers for multilayers fabricated through (red) conventional LbL assembly dipping method and LbL assembly under high gravity field (black line), respectively.

dipping process, the deposition time of PAzo during LbL assembly with PDDA was determined through its adsorption kinetics on substrate modified with PDDA through stepwise characterization of UV−visible spectra to trace the deposited amount of PAzo after immersing for a certain time interval. The PAzo solution displayed three-featured absorption (Figure 1a): a strong peak with the maximum absorbance at around 357 nm, which was assigned to $\pi-\pi^*$ transition of trans-azobenzene, an accompanying small peak at 266 nm attributed to the electronic transition parallel to the short axis of the trans-azobenzene molecule, and a relatively weak broad absorption at around 450 nm which indicated the presence of n-π^* transition of cis-azobenzene molecule.[43] The absorbance of the maximum featured peak was used to monitor the amount of PAzo deposited on the substrate, which was plotted versus the immersion time. As shown in Figure 1b, the amount of deposited PAzo grew rapidly at an early stage, and then the rate of increase gradually slowed and finally reached a constant value after about 12 min, indicating saturated adsorption of PAzo. Bearing in mind the possible large fluctuation of adsorbed PAzo during the period of rapid increase before 12 min, the time for the deposition of PAzo in the further LbL assembly process should be determined as 15 min or even longer, which seemed time-consuming and tedious.

To shorten this procedure, we applied the high gravity field to the adsorption kinetics of PAzo by exposing the substrate with PDDA to PAzo solutions with different time interval in the presence of high gravity field. As shown in Figure 1b, the time to reach saturated adsorption was shortened to 4 min, 2 min, and 30 s at rotating speeds of 1800, 2400, and 3000 r/min, respectively. Meanwhile, the adsorbed saturated values of PAzo were similar to those deposited under the conventional LbL assembly process. These phenomena suggested that the high gravity field was effective in accelerating the adsorption process of PAzo molecules, which demonstrated a maximum increase of deposition efficiency as high as 20-fold while retaining a comparable amount of saturated adsorption; the effects of acceleration became more remarkable with the strength of the applied high gravity field indicated by the correlation of adsorption kinetics and its increasing rotating speed. Due to the acceleration effects of the high gravity field, even the building block solution with an extremely low concentration could realize rapid adsorption onto the substrate and fast LbL assembly process. In this way, the consumption of building block solution could be lowered in LbL assembly, which should be meaningful for the fabrication of multilayers with expensive and rare species, such as proteins. For conventional adsorption in solution, the low concentration decreased the driving forces for adsorption and thus would be time-consuming to reach saturated adsorption. For conventional dipping LbL assembly, the time to reach saturated adsorption was 10, 12, and 20 min from PAzo concentrations of 0.02, 0.01, and 0.005 mg/mL, respectively (Figure 2). Under the same conditions, the high gravity shortened the required saturated adsorption time to 1.5, 3, and 4 min, which was about 5−7 times less than under normal conditions. The mechanism for rapid adsorption in the presence of a high gravity field was attributed to the thinned fluidic boundary layer interfering with the diffusion layer, which reduced fluidic resistance and thus enhanced the adsorption process at the interface as seen in our previous report.[40−42]

Although the adsorption kinetics have proven faster in the high gravity field than under conventional dipping, the LbL assembling behavior between PDDA and PAzo must still to be checked for film increasing condition and film quality. For comparison,we carried out the dipping LbL assembly of PDDA and PAzo by alternately immersing the quartz substrate in PDDA (aq, 1 mg/mL) for 10 min and PAzo (aq, 0.01 mg/mL) for 15 min. The LbL assembly process was monitored by UV−

DOI: 10.1021/acsami.5b02179
ACS Appl. Mater. Interfaces 2015, 7, 10920−10927

visible spectra after each deposition of PAzo, as summarized in Figure 3a. With the increasing number of deposited PDDA/PAzo bilayers, the maximum featured peak increased linearly, which indicated a constant content of PAzo in every deposited bilayer; in addition, this maximum peak red-shifted by 13.5 nm (Part 2 of Supporting Information), which might be caused by both environmental effect and J-like aggregation of azobenzene molecules in the multilayer.[43] After applying a high gravity field to the LbL assembly process (Scheme 1), the alternate deposition of PDDA and PAzo was realized through alternate pumping solutions of PDDA (aq, 1 mg/mL) for 1 min and PAzo (aq, 0.01 mg/mL) for 3 min each, which was sufficient to reach saturated adsorption. Between every deposition, the substrates fixed within the high gravity equipment were washed by pumping deionized water three times, each followed by drying by rotating the equipment without any solutions. The rotating speed was fixed at 2400 r/min for all experiments if not otherwise specifically noted. The LbL assembling behavior demonstrated in Figure 3b was similar to that under the conventional dipping process, which demonstrated a linear increase with the deposition of the PDDA/PAzo bilayer, as summarized in Figure 3c. The maximum featured peak at around 370 nm red-shifted by 5 nm, caused by the presence of a J-like aggregation of azobenzene groups.[43,44] These phenomena demonstrated that the similar LbL assembling behaviors of PDDA/PAzo were almost not influenced by introducing high gravity field.

As we can see from Figure 3c, the film deposited under a high gravity field had a much lower absorbance than that under the conventional dipping method. This could be the result of either a smaller deposited amount of PAzo in every bilayer or by a thinner and more compact film fabricated under high gravity. Since the adsorption kinetics in Figure 1 revealed that the saturated adsorption of PAzo onto PDDA for one bilayer was similar under the conventional LbL dipping assembly process and a high gravity field, we can exclude the possibility of less deposited PAzo in every bilayer. To check the film compactness and confirm the second possibility, we investigated the surface morphology of the $(PDDA/PAzo)_5$ multilayer through AFM images at different concentrations, both under dipping conditions and a high gravity field. For the LbL assembly process under conventional dipping, the PDDA/PAzo multilayer displayed a compact and homogeneous particle-like surface morphology as shown in Figure 4. The surface roughness was dependent on the concentration of PAzo solution and presented a decreasing value from 2.6 nm at 0.02 mg/mL and 2.0 nm at 0.01 mg/mL to 1.6 nm at 0.005 mg/mL, during which the surface grew smoother and more close-packed (Figure 4a–c). Under the same corresponding concentration conditions in the presence of a high gravity field, the surface roughness of the PDDA/PAzo multilayers dropped to 2.2 nm at 0.02 mg/mL, 1.7 nm at 0.01 mg/mL and 1.2 nm at 0.005 mg/mL, which were lower than those at the same corresponding number of bilayer under the conventional dipping method (Part 3 of Supporting Information). There were also few observable aggregates on the surface, which meant smooth and compact film morphology. To figure out the reason for difference in surface roughness, we have measured the film thickness with ellipsometer and found that for $(PDDA/PAzo)_5$ and $(PDDA/PAzo)_{10}$ multilayers fabricated under conventional dipping assembly, the film thickness was 18.9 ± 0.2 and 10.2 ± 0.5 nm, respectively; for $(PDDA/PAzo)_5$ and $(PDDA/PAzo)_{10}$ multilayers prepared through LbL assembly under high gravity field, the film thickness reduced to 10.3 ± 1.0 and 4.6 ± 0.1 nm, correspondingly. The reduced film thickness supported the reduced surface roughness under high gravity field to some degree. Moreover, the difference in surface roughness revealed from AFM images matched well with the absorbance difference of PDDA/PAzo multilayers fabricated through the conventional LbL dipping assembly method and LbL assembly under a high gravity field. With much surface roughness, the rough structures contributed to the strong scattering and absorption of light irradiation, leading to thoroughly higher absorbance values of the multilayer assembled through the dipping method than those of the multilayer assembled under high gravity in the UV–visible spectra, as shown in Figure 3c.

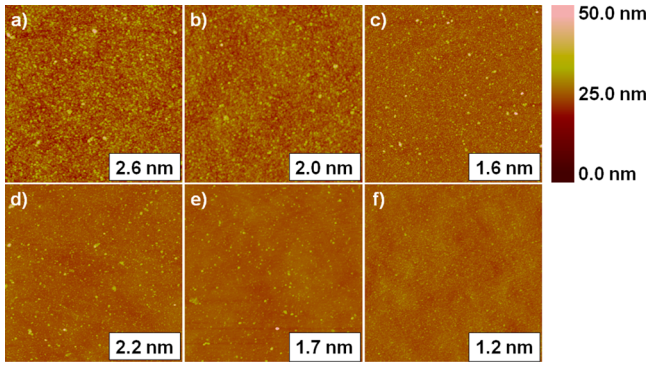

Figure 4. AFM images of $(PDDA/PAzo)_5$ multilayer fabricated through the conventional dipping LbL assembly process at (a) 0.02, (b) 0.01, and (c) 0.005 mg/mL, and through LbL assembly under high gravity field at (d) 0.02, (e) 0.01, and (f) 0.005 mg/mL. The displayed images are 5×5 μm scans. The numbers at the right corner of each AFM are corresponding surface roughness of the displayed AFM image.

Although the film presented homogeneous compactness as seen from AFM images, we wondered whether it exhibited lowered ion permeability in the presence of a high gravity field. The permeability of cation and anion through the as-prepared PDDA/PAzo multilayer was characterized with CV curves via the electrochemical probing of negatively charged $[Fe(CN)_6]^{3-}$ label and positively charged $[Ru(NH_3)_6]^{3+}$, respectively. The $(PDDA/PAzo)_{10}$ multilayers were fabricated on pretreated gold electrode with mercaptoacetic acid groups and tested with CV methods with an electrochemical workstation. We consider that the multilayer formation on gold electrode substrate should be comparable with that on quartz substrate because the LbL assembly has been generally accepted as a versatile method independent of substrate quality, shape, and size. Typical CV curves of bare electrode, and electrode with a PDDA/PAzo multilayer fabricated through LbL assembly under both conventional dipping and high gravity field are shown in Figure 5a for anion label and Figure 5b for cation label. The closed CV loop of the electrode modified with $(PDDA/PAzo)_{10}$ multilayer demonstrated that the redox response for the $[Fe(CN)_6]^{3-}$ or $[Ru(NH_3)_6]^{3+}$ decreased compared with that before modification, which indicated that the presence of a PDDA/PAzo multilayer lowered the permeability of cation or anion on the electrode. Meanwhile, when introducing a high gravity field for the LbL deposition of $(PDDA/PAzo)_{10}$ multilayer, the redox response of the cation or anion probing declined to a lower level than that for conventional LbL assembled film, as we could see the decreased area of the CV

DOI: 10.1021/acsami.5b02179
ACS Appl. Mater. Interfaces 2015, 7, 10920–10927

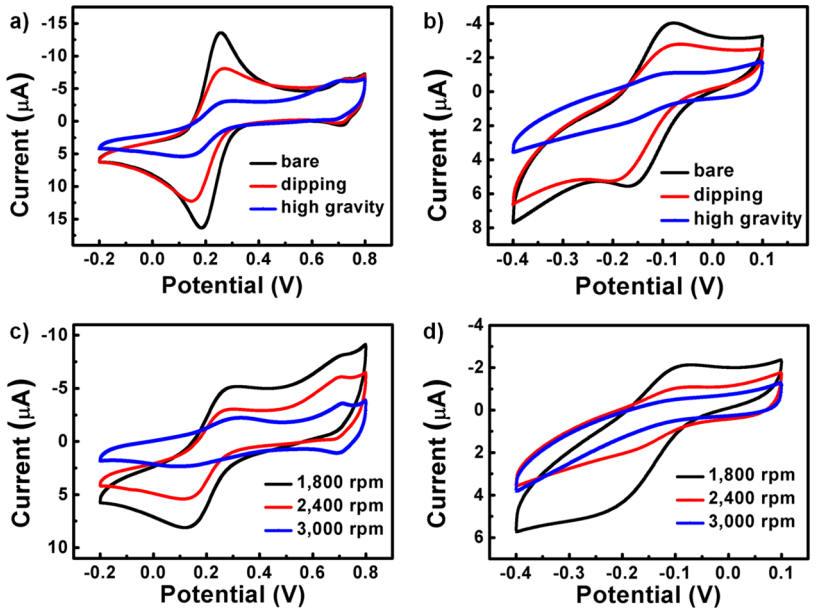

Figure 5. CV curves of (black) bare electrode, (red) electrode with $(PDDA/PAzo)_{10}$ multilayer fabricated through conventional dipping LbL assembly, and (blue) LbL assembly under high gravity field in the presence of (a) $K_3[Fe(CN)_6]$ anion label and (b) $[Ru(NH_3)_6]Cl_3$ cation label. CV curve electrodes with $(PDDA/PAzo)_{10}$ multilayer fabricated through LbL under high gravity field with different rotating speeds of (black)1800, (red) 2400, and (blue) 3000 r/min detected with (c) $K_3[Fe(CN)_6]$ anion label and (d) $[Ru(NH_3)_6]Cl_3$ cation label.

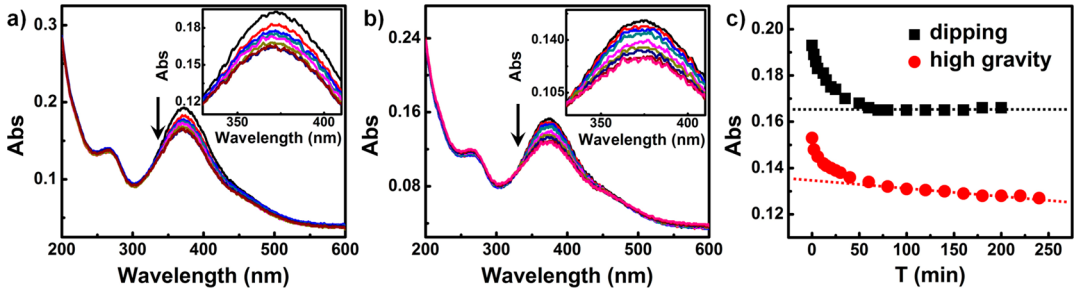

Figure 6. Stepwise UV−visible spectra of $(PDDA/PAzo)_7$ multilayers fabricated under (a) conventional LbL dipping assembly method and (b) high gravity field after exposure to UV irradiation for certain time intervals; (insets) corresponding local magnification at the maximum featured peak. (c) Photoisomerization kinetics in (black ■) panel a and (red ●) panel b were compared.

loop, which suggested the increased compactness of the multilayer and enhanced ion blocking effects of the multilayer. These results for ion permeability on multilayers prepared under the conventional dipping condition or a high gravity field matched well with the surface morphology and surface roughness revealed from AFM images.

To further demonstrate the adjusting property of a high gravity field over the compactness of the LbL assembled multilayers, we further characterized the cation and anion permeability of the $(PDDA/PAzo)_{10}$ multilayer in the presence of the high gravity field with rotating speeds of 1800, 2400, and 3000 r/min. For the anion permeability in Figure 5c, the area of the closed loops formed by the CV curves gradually decreased with the increasing rotational speed of the high gravity equipment, suggesting reduced ion permeability. For the cation permeability in Figure 5d, similarly, the redox response of the $(PDDA/PAzo)_{10}$ multilayer decreased and resulted in a lowering area of closed CV loops as the rotating speed grew. These results support the idea that the high gravity field in the LbL assembling process was effective in increasing the ion blocking property of the LbL assembled multilayers through control over the rotating speed of the equipment.

To understand the increased compactness of the multilayer after introducing a high gravity field, we compared the kinetics of the photoinitiated conformation changes of the azobenzene groups within the PDDA/PAzo multilayers fabricated through LbL assembly under both conventional dipping and the high gravity field. Generally, azobenzene groups are known to exhibit reversible conformation changes between cis-form and trans-form in response to UV irradiation and visible light, correspondingly. We therefore detected the photo responsive conformation changes of $(PDDA/PAzo)_7$ multilayers through UV−visible spectra after exposing the multilayers to UV light at a wavelength of 375 nm with an intensity of 3 mW/cm^2. Under dark conditions, there was feature absorption at 372 nm attributed to $\pi-\pi$ stacking interactions of trans-azobenzene; after exposure to UV light for a certain period, this featured peak gradually declined. The decrease in absorbance at 372 nm was traced to characterize transformation kinetics of the above conformation changes; the absorbance values versus the time exposed to UV light were plotted in Figure 6. For the PDDA/PAzo multilayer fabricated through conventional LbL assembly process (Figure 6a,c), the absorbance underwent a rapid drop in the early 20 min, a slow decrease in the later 50 min, and

DOI: 10.1021/acsami.5b02179
ACS Appl. Mater. Interfaces 2015, 7, 10920−10927

almost reached a constant after exposure to UV light for a total 70 min. Within the loosely packed multilayers, the azobenzene groups had sufficient space for rapid transformation and isomerization from *trans*-form to *cis*-form. For the PDDA/PAzo multilayer prepared under high gravity field, however, the isomerization kinetics grew longer (Figure 6b,c). The decrease of absorbance at 380 nm slowed remarkably after almost 20 min, and continued decreasing slightly. Even at 240 min, the absorbance decrease did not reach a constant value, indicating that isomerization still slowly continued. This result was caused by the difficulty of isomerization within a highly limited small space resulting from compact and closely packed structures of the PDDA/PAzo multilayer fabricated under the high gravity field. The remarkable difference in the time to complete the photoinitiated conformation changes of azobenzene demonstrated difference in the available space within the two kinds of multilayers fabricated under dipping and the high gravity field, further supporting the greatly increased film compactness of the PDDA/PAzo multilayer after introducing the high gravity field. The above phenomena corresponded well with the results obtained from the surface morphology and ion permeability of the PDDA/PAzo multilayers prepared under conventional dipping conditions and a high gravity field. To this end, the involvement of simple mechanical energy in the LbL assembling process did have an effect in refining multilayer structures and improving film compactness, which was realized by the strong shear forces provided by the high gravity field to strongly orientate the deposited molecules.

CONCLUSIONS

To summarize, we have achieved control over film compactness and ion permeability of LbL assembled multilayers through introducing a process intensification method of high gravity field. By taking the PDDA/PAzo multilayer as a model system, we have demonstrated accelerated effect of high gravity field on the film formation by the maximum 20-fold and improved film quality with lower surface roughness, smoother morphology, and more compact film structures. These results were supported by AFM images, CV curves, and photoisomerization kinetics of azobenzene molecules when compared with the multilayers fabricated under conventional dipping method. Moreover, the film compactness and ion permeability of the multilayer could be well tailored through the rotating speed of the high gravity field, thus providing a simple and versatile mechanical energy in LbL assembly to adjust film properties of nanothin multilayers, which could be useful for further industrialized applications in controlled ion permeability, anticorrosion, and drug loading.

ASSOCIATED CONTENT

Supporting Information

Detailed description of high gravity technique, red-shift of PDDA/PAzo multilayers, and stepwise characterization of surface morphology of PDDA/PAzo multilayers. The Supporting Information is available free of charge on the ACS Publications website at DOI: 10.1021/acsami.5b02179.

AUTHOR INFORMATION

Corresponding Authors

*E-mail: shi@mail.buct.edu.cn,
*E-mail: shaol@mail.buct.edu.cn.

Author Contributions

The manuscript was written through contributions of all authors. All authors have given approval to the final version of the manuscript.

Notes

The authors declare no competing financial interest.

ACKNOWLEDGMENTS

This work was supported by NSFC (21374006; 51422302), the Program of the Co-Construction with Beijing Municipal Commission of Education of China, Open Project of State Key Laboratory of Supramolecular Structure and Materials (SKLSSM2015017), and Beijing Young Talents Plan (YETP0488). We thank Dr. Dengli Qiu from Bruker (Beijing) Scientific Technology Co., Ltd., for his kind help of AFM test and analysis.

REFERENCES

(1) Iler, R. K. Multilayers of Colloidal Particles. *J. Colloid Interface Sci.* **1966**, *21*, 569−594.
(2) Decher, G. Fuzzy Nanoassemblies: Toward Layered Polymeric Multicomposites. *Science* **1997**, *277*, 1232−1237.
(3) Decher, G.; Hong, J. D. Buildup of Ultrathin Multilayer Films by a Self-Assembly Process: 1. Consecutive Adsorption of Anionic and Cationic Bipolar Amphiphiles on Charged Surfaces. *Makromol. Chem., Macromol. Symp.* **1991**, *46*, 321−327.
(4) Zhang, X.; Chen, H.; Zhang, H. Y. Layer-by-Layer Assembly: From Conventional to Unconventional Methods. *Chem. Commun.* **2007**, 1395−1405.
(5) Zhang, X. Surface Molecular Engineering of Polymer Multilayer Films. *Acta Polym. Sin.* **2007**, *1*, 905−912.
(6) Li, H. L.; Pang, S. P.; Wu, S.; Feng, X. L.; Müllen, K.; Bubeck, C. Layer-by-Layer Assembly and UV Photoreduction of Graphene-Polyoxometalate Composite Films for Electronics. *J. Am. Chem. Soc.* **2011**, *133*, 9423−9429.
(7) Jiang, C.; Cheng, M. J.; Liu, H. T.; Shao, Lei.; Zeng, X. F.; Zhang, Y. J.; Shi, F. Fabricating Transparent Multilayers with UV and Near-IR Double-Blocking Properties through Layer-by-Layer Assembly. *Ind. Eng. Chem. Res.* **2013**, *52*, 13393−13400.
(8) Cheng, M. J.; Shi, F.; Li, J. S.; Lin, Z. F.; Jiang, C.; Xiao, M.; Zhang, L. Q.; Yang, W. T.; Nishi, T. Macroscopic Supramolecular Assembly of Rigid Building Blocks through a Flexible Spacing Coating. *Adv. Mater.* **2014**, *26*, 3009−3013.
(9) Cheng, M. J.; Liu, Q.; Xian, Y. M.; Shi, F. Programmable Macroscopic Supramolecular Assembly through Combined Molecular Recognition and Magnetic Field-Assisted Localization. *ACS. Appl. Mater. Interfaces* **2014**, *6*, 7572−7578.
(10) Li, Y.; Li, L.; Sun, J. Q. Bioinspired Self-Healing Superhydrophobic Coatings. *Angew. Chem., Int. Ed.* **2010**, *49*, 6129−6133.
(11) Guo, C. X.; Zheng, X. T.; Lu, Z. S.; Luo, X. W.; Li, C. M. Biointerface by Cell Growth on Layered Graphene−Artificial Peroxidase−Protein Nanostructure for in Situ Quantitative Molecular Detection. *Adv. Mater.* **2010**, *22*, 5164−5167.
(12) Städler, B.; Price, A. D.; Chandrawati, R.; Rigau, L. H.; Zelikina, A. N.; Caruso, F. Polymer Hydrogel Capsules: en Route toward Synthetic Cellular Systems. *Nanoscale* **2009**, *1*, 68−73.
(13) Yin, S. Y.; Niu, Z. Q.; Chen, X. D. Assembly of Graphene Sheets into 3D Macroscopic Structures. *Small* **2012**, *8*, 2458−2463.
(14) Niu, Z. Q.; Du, J. J.; Cao, X. B.; Sun, Y. H.; Zhou, W. Y.; Hng, H. H.; Ma, J.; Chen, X. D.; Xie, S. S. Electrophoretic Buildup of Alternately Multilayered Films and Micro-Patterns Based on Graphene Sheets and Nanoparticles and their Applications in Flexible Supercapacitors. *Small* **2012**, *8*, 3201−3208.
(15) Podsiadlo, P.; Kaushik, A. K.; Arruda, E. M.; Waas, A. M.; Shim, B. S.; Xu, J. D.; Nandivada, H.; Pumplin, B. G.; Lahann, J.; Ramamoorthy, A.; Kotov, N. A. Ultrastrong and Stiff Layered Polymer Nanocomposites. *Science* **2007**, *318*, 80−83.

(16) Yu, Y.; Zhang, H.; Cui, S. X. Fabrication of Robust Multilayer Films by Triggering the Coupling Reaction Between Phenol and Primary Amine Groups with Visible Light Irradiation. *Nanoscale* **2011**, *3*, 3819−3824.
(17) Zhou, Y.; Cheng, M. J.; Zhu, X. Q.; Zhang, Y. J.; An, Q.; Shi, F. A Facile Method to Prepare Molecularly Imprinted Layer-by-Layer Nanostructured Multilayers Using Postinfiltration and a Subsequent Photo-Cross-Linking Strategy. *ACS. Appl. Mater. Interfaces* **2013**, *5*, 8308−8313.
(18) Wang, Y. F.; Wang, S. J.; Xiao, M.; Han, D. M.; Hickner, M. A.; Meng, Y. Z. Layer-by-Layer Self-Assembly of PDDA/PSS-SPFEK Composite Membrane with Low Vanadium Permeability for Vanadium Redox Flow Battery. *RSC Adv.* **2013**, *3*, 15467−15474.
(19) Lu, H. Y.; Hu, N. F. Salt-Induced Swelling and Electrochemical Property Change of Hyaluronic Acid/Myoglobin Multilayer Films. *J. Phys. Chem. B* **2007**, *111*, 1984−1993.
(20) Chan, E. P. Deswelling of Ultrathin Molecular Layer-by-Layer Polyamide Water Desalination Membranes. *Soft Matter* **2014**, *10*, 2949−2954.
(21) Jin, W. Q.; Toutianoush, A.; Tieke, B. Use of Polyelectrolyte Layer-by-Layer Assemblies as Nanofiltration and Reverse Osmosis Membranes. *Langmuir* **2003**, *19*, 2550−2553.
(22) Yang, M.; Lu, S. F.; Lu, J. L.; Jiang, S. P.; Xiang, Y. Layer-by-Layer Self-Assembly of PDDA/PWA−Nafion Composite Membranes for Direct Methanol Fuel Cells. *Chem. Commun.* **2010**, *46*, 1434−1436.
(23) Liu, D. S.; Ashcraft, J. N.; Mannarino, M. M.; Silberstein, M. N.; Argun, A. A.; Rutledge, G. C.; Boyce, M. C.; Hammond, P. T. Spray Layer-by-Layer Electrospun Composite Proton Exchange Membranes. *Adv. Funct. Mater.* **2013**, *23*, 3087−3095.
(24) Yang, Y.-H.; Bolling, L.; Priolo, M. A.; Grunlan, J. C. Super Gas Barrier and Selectivity of Graphene Oxide-Polymer Multilayer Thin Films. *Adv. Mater.* **2013**, *25*, 503−508.
(25) Aulin, C.; Karabulut, E.; Tran, A.; Wågberg, L.; Lindström, T. Transparent Nanocellulosic Multilayer Thin Films on Polylactic Acid with Tunable Gas Barrier Properties. *ACS Appl. Mater. Interfaces* **2013**, *5*, 7352−7359.
(26) Itoh, Y.; Matsusaki, M.; Kida, T.; Akashi, M. Locally Controlled Release of Basic Fibroblast Growth Factor from Multilayered Capsules. *Biomacromolecules* **2008**, *9*, 2202−2206.
(27) Wang, L.; Wang, X.; Xu, M. F.; Chen, D. D.; Sun, J. Q. Layer-by-Layer Assembled Microgel Films with High Loading Capacity: Reversible Loading and Release of Dyes and Nanoparticles. *Langmuir* **2008**, *24*, 1902−1909.
(28) Andreeva, D. V.; Skorb, E. V.; Shchukin, D. G. Layer-by-Layer Polyelectrolyte/Inhibitor Nanostructures for Metal Corrosion Protection. *ACS Appl. Mater. Interfaces* **2010**, *2*, 1954−1962.
(29) Pardo-Yissar, V.; Katz, E.; Lioubashevski, O.; Willner, I. Layered Polyelectrolyte Films on Au Electrodes: Characterization of Electron-Transfer Features at the Charged Polymer Interface and Application for Selective Redox Reactions. *Langmuir* **2001**, *17*, 1110−1118.
(30) Farhat, T. R.; Schlenoff, J. B. Ion Transport and Equilibria in Polyelectrolyte Multilayer. *Langmuir* **2001**, *17*, 1184−1192.
(31) Chia, K.-K.; Rubner, M. F.; Cohen, R. E. pH-Responsive Reversibly Swellable Nanotube Arrays. *Langmuir* **2009**, *25*, 14044−14052.
(32) Tan, W. S.; Cohen, R. E.; Rubner, M. F.; Sukhishvili, S. A. Temperature-Induced, Reversible Swelling Transitions in Multilayers of a Cationic Triblock Copolymer and a Polyacid. *Macromolecules* **2010**, *43*, 1950−1957.
(33) Kumar, S. K.; Hong, J.-D. Photoresponsive Ion Gating Function of an Azobenzene Polyelectrolyte Multilayer Spin-Self-Assembled on a Nanoporous Support. *Langmuir* **2008**, *24*, 4190−4193.
(34) Ma, Y. J.; Dong, W.-F.; Hempenius, M. A.; Möhwald, H.; Vancso, G. J. Redox-Controlled Molecular Permeability of Composite-Wall Microcapsules. *Nat. Mater.* **2006**, *5*, 724−729.
(35) Ge, L.; Wu, L.; Wu, B.; Wang, G. H.; Xu, T. W. Preparation of Monovalent Cation Selective Membranes through Annealing Treatment. *J. Membr. Sci.* **2014**, *459*, 217−222.
(36) Xu, W.; Choi, I.; Plamper, F. A.; Synatschke, C. V.; Müller, A. H. E.; Tsukruk, V. V. Nondestructive Light-Initiated Tuning of Layer-by-Layer Microcapsule Permeability. *ACS Nano* **2013**, *7*, 598−613.
(37) Huang, C.-J.; Chang, F.-C. Using Click Chemistry to Fabricate Ultrathin Thermoresponsive Microcapsules through Direct Covalent Layer-by-Layer Assembly. *Macromolecules* **2009**, *42*, 5155−5166.
(38) Bernsmann, F.; Ersen, O.; Voegel, J.-C.; Jan, E.; Kotov, N. A.; Ball, V. Melanin-Containing Films: Growth from Dopamine Solutions versus Layer-by-Layer Deposition. *ChemPhysChem* **2010**, *11*, 3299−3305.
(39) Fu, Y.; Li, S.-J.; Xu, J.; Yang, M.; Zhang, J.-D.; Jiao, Y.-H.; Zhang, J.-C.; Zhang, K.; Jia, Y.-G. Facile and Efficient Approach to Speed up Layer-by-Layer Assembly: Dipping in Agitated Solutions. *Langmuir* **2011**, *27*, 672−677.
(40) Ma, L. X.; Cheng, M. J.; Jia, G. J.; Wang, Y. Q.; An, Q.; Zeng, X. F.; Shen, Z. G.; Zhang, Y. J.; Shi, F. Layer-by-Layer Self-Assembly under High Gravity Field. *Langmuir* **2012**, *28*, 9849−9856.
(41) Liu, X. L.; Luo, C. J.; Jiang, C.; Shao, L.; Zhang, Y. W.; Shi, F. Rapid Multilayer Construction on non-Planar Substrate by Layer-by-Layer Self-Assembly under High Gravity. *RSC Adv.* **2014**, *4*, 59528−59534.
(42) Jiang, C.; Liu, X. L.; Luo, C. J.; Zhang, Y. J.; Shao, L.; Shi, F. Controlled Exponential Growth in Layer-by-Layer Multilayers Using High Gravity Fields. *J. Mater. Chem. A* **2014**, *2*, 14048−14053.
(43) Dante, S.; Advincula, R.; Frank, C. W.; Stroeve, P. Photoisomerization of Polyionic Layer-by-Layer Films Containing Azobenzene. *Langmuir* **1999**, *15*, 193−201.
(44) Rau, H. In *Photoisomerization of Azobenzenes in Photochemistry and Photophysics*; Rabek, J. F., Ed.; CRC Press: Boca Raton, FL, 1990; Vol. *II*, pp 119−141.

DOI: 10.1021/acsami.5b02179
ACS Appl. Mater. Interfaces 2015, 7, 10920−10927